Giant resonance effects in the electron-impact ionization of heavy atoms and ions

Stephen M. Younger
A-Division, Lawrence Livermore National Laboratory, Livermore, California 94550
(Received 15 September 1986)

The origin of giant resonance effects in the electron-impact ionization of heavy ($Z > 50$) atoms and ions is discussed in terms of the potentials governing the scattering states. Calculations are presented for electron-impact ionization of the $4d$ subshell in Xe, Cs^+, Ba^{2+}, Xe^+, and I^+, and for ionization of the $4f$ subshell in Eu^+, Tm^+, Yb^{2+}, Lu^{3+}, and W^+.

I. INTRODUCTION

The study of electron scattering from heavy atoms and ions offers rich rewards in terms of the range and complexity of the phenomena revealed. Although there has been much information published regarding both elastic and inelastic electron scattering from heavy neutral atoms,[1] especially the noble gases, relatively little definitive work has been done on inelastic processes in ions. Over the past few years, however, stable and well-characterized ion sources have become available which have allowed a variety of crossed electron-ion beam measurements to be made on the electron-impact-ionization cross sections of singly and multiply charged ions, including several heavy ions.[2]

Some of the recent measurements of heavy ions have revealed the presence of large anomalous features in the cross section at relatively low incident electron energies (less than two times the threshold energy). Recently, one such feature in Cs^+ has been interpreted as a giant scattering resonance appearing in the scattered electron channel.[3] This was the first identification of a true giant shape resonance occurring in an inelastic scattering of electrons from ions. The present paper gives further details of the computational method employed in distorted-wave calculations of giant resonance phenomena and presents the results of similar calculations for a number of additional examples. Section II gives a brief summary of the theory of giant resonances in electron-ion scattering and the computational method employed to compute the cross section. Section III presents results for Xe, Cs^+, Ba^{2+}, La^{3+}, Xe^+, I^+, Tm^+, Yb^{2+}, Lu^{3+}, Eu^+, and W^+. Section IV summarizes the work and suggests opportunities for further calculations and measurements.

II. THEORY

A. Giant resonances

It has been known at least since Hartree's first paper on the self-consistent-field method[4] that the potential describing high-angular-momentum states in heavy atoms can have a double-well character, consisting of a deep inner well dominated by the nuclear charge and centrifugal force, a potential barrier at intermediate radii arising from the localized charge density of many-electron subshells, and an outer well which eventually approaches the asymptotic Coulomb potential of the ion. If the inner potential well is sufficiently wide and deep, it can support bound states. All of the atomic core electrons and the inner nodes of most excited orbitals reside in the vicinity of this inner well. For higher-angular-momentum ($l \geq 3$ for $Z \geq 50$) excited-state orbitals the inner potential well may be too narrow to support a bound state. In such cases the bound states of the symmetry all occur in the outer potential well, having much larger mean radii than the compact core orbitals. The resulting small overlap between outer-well excited-state orbitals and the inner-well core orbitals can have profound effects on a variety of atomic excitation processes including photoabsorption and electron scattering.[5]

Even if the inner potential well is not capable of supporting a true negative-energy bound state, it may still exhibit a quasibound-state behavior which can dramatically affect collisional properties. Consider a scenario common for heavy atoms where the potential describing excited f states has a double-well character with an intermediate potential barrier extending above zero potential energy. If the positive maximum of the potential barrier is artificially continued to $r = \infty$, the resulting modified potential well may support one or more bound states at *positive* energy. Such states are compact, i.e., they reside in the original inner well, and thus have large overlaps with core orbitals. As this artificial continuation of the potential barrier to large radii is relaxed so as to recover the actual potential, such pseudobound states will tunnel through the barrier and will cease to be true localized bound states. Continuum waves at energies near those of pseudobound states will, however, experience a sudden increase in orbital probability density in the vicinity of the inner well. It is this sudden increase in inner-well continuum orbital density that is responsible for giant resonances to appear in cross sections describing the interaction of inner-shell bound orbitals with continuum states. Note that the existence of such virtual resonance states in heavy atoms is analogous to scattering from a simple square-well potential, as has been shown by Connerade.[6] Such an analogy demonstrates that the occurrence of virtual resonance states in the inner potential well is not determined so much by the amplitude of the potential barrier as by the product of the effective depth of the inner well and the square of its width. It is the sensitivity of the inner-well

 ©1987 The American Physical Society

potential to the structure of the ion that makes it difficult to establish *a priori* rules for the occurrence of resonant scattering states.

It is important to remember that shape resonances differ from excitation-autoionization resonances which commonly occur[2] in electron-impact ionization. The latter are compound resonances, in that a continuum wave mixes with a localized autoionizing state with which it is degenerate. Shape resonances occur because of the particular properties of the partial wave potentials and do not necessarily have large mixing coefficients with other localized configurations.

The transfer of continuum orbital density from the outer well into the inner potential well is reflected in the phase shift of the partial wave, a measure of continuum orbital penetration into the non-Coulombic atomic core. As a shape resonance is traversed, the phase shift of the partial wave increases by π, indicating the addition of a node to the orbital in the vicinity of inner well. Figure 1 illustrates this phenomenon for f-wave scattering from Cs^+. As the phase shift increases by π in going through the shape resonance, the innermost portion of the continuum orbital gains a node. In some cases, such as low-

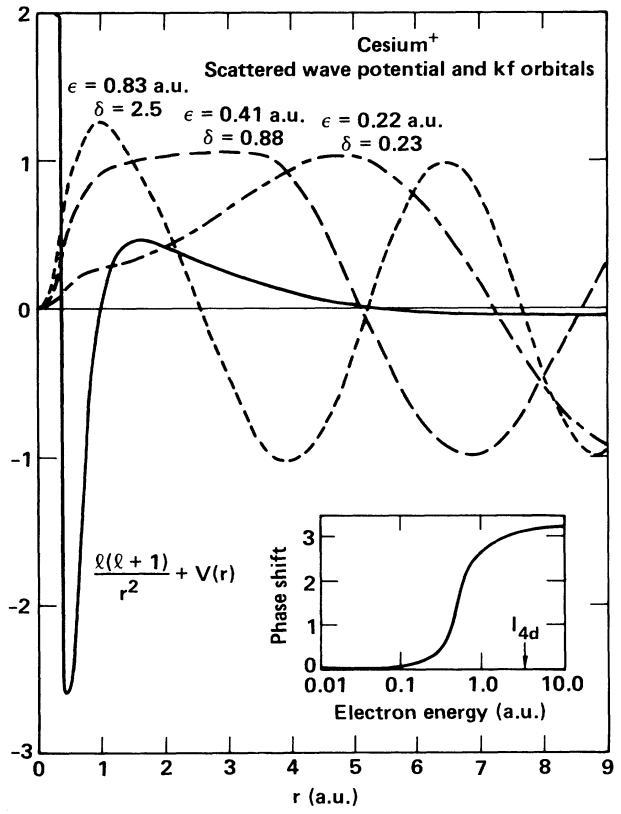

FIG. 1. Scattering potential for the incident and scattered channels of Cs^+ in atomic units (——). Note the strong potential barrier separating the inner and outer potential wells. The dashed curves correspond to kf partial waves computed in this potential, illustrating the formation of an additional node as the scattering resonance is traversed. The inset shows the phase shift as a function of energy.

energy electron scattering from neutral atoms, several resonances may be supported by the potential, resulting in several additions of π to the phase shift. Mott and Massey[1] have related the quantity $2h(\partial\delta/\partial E)$, where h is Plank's constant and $\partial\delta/\partial E$ is the slope of the phase shift with respect to the energy, to the time delay experienced by the electron in the scattering event. Substituting typical values of the slope at the center of an f-wave resonance in heavy ions, we obtain a delay of only 10^{-15} sec—well below measurable time scales.

We distinguish between two mechanisms by which such potential barriers can be created in heavy atoms, one of which is due to the direct part of the electrostatic potential generated by the core electrons and the other of which is primarily an electron exchange effect. An example of the former is f-wave scattering from noble gas atoms and ions, such as Cs^+, where the potential barrier is created by the localized charge density of the 18 electrons in the $4s$, $4p$, and $4d$ subshells. A second mechanism for the formation of strong potential barriers in heavy atoms arises from exchange interactions which occur between the core and the excited orbitals. These interactions are highly dependent on the specific angular term value within the excited configuration. An inspection of the angular coefficients determining the atomic Hamiltonian[7] shows that such term dependence is most pronounced for configurations of the type $nl^{4l+1}kl'$.[7] As an important example, the interaction between a d^9 subshell and an excited f electron is (in a.u.)

$$E_{\rm av}-(8/35)F^2-(2/21)F^4-(3/70)G^1-(2/105)G^3-(5/231)G^5 \quad (1)$$

in the ^3P configuration and

$$E_{\rm av}-(8/35)F^2-(2/21)F^4+(137/70)G^1-(2/105)G^3-(5/231)G^5 \quad (2)$$

in the ^1P configuration. Here $E_{\rm av}$ is the average energy of the configuration (Ref. 7), F^k is the direct electrostatic integral

$$F^k=\int\int P_d(r)P_d(r)(1/r_{12})P_f(r')P_f(r')dr\,dr' \quad (3)$$

and G^k is the exchange integral

$$G^k=\int\int P_d(r)P_d(r')(1/r_{12})P_f(r)P_f(r')dr\,dr' . \quad (4)$$

$P_d(r)$ and $P_f(r)$ are the radial orbitals corresponding to the d and f states, respectively. The large coefficient of the exchange integral in (2) is characteristic of singlet terms in configurations involving a single electron outside an almost-filled subshell and has been found to be very important in determining both bound-bound[8] and bound-continuum[9–11] properties in heavy atoms.

B. Computational method

The general features of the distorted-wave Born-exchange method used in the present paper have been discussed in detail in several previous publications[12,13] and will only be summarized here. The cross section is described by a triple partial-wave expansion over the in-

cident, scattered, and ejected (originally bound) channels. A Gaussian integration is performed over the possible distribution of final-state energy between the two continuum electrons. Exchange between the two final-state electrons is approximated by the "maximum interference" approximation of Peterkop.[14]

Target orbitals were computed using the Hartree-Fock code of Fischer.[15] Bound orbitals corresponding to the initial ion ground state were used in all phases of the calculations. Unless otherwise stated, the ionization energies were computed as the difference between the state specific Hartree-Fock total energies of the initial ground state and the final hole state of the ionized system.

The potentials used to generate the continuum scattering orbitals were constructed as follows: The initial and scattered channels were computed in the field of the initial ion. The ejected continuum waves were computed in the potential of the residual ion, i.e., the initial ion minus the electron which is removed. Unless otherwise indicated, a local semiclassical exchange (SCE) approximation[16] to the Hartree-Fock potential was employed in the partial-wave calculations. In previous studies[11,13] this form of the scattering potential has been found to yield continuum orbitals in remarkable agreement with those computed in the actual nonlocal Hartree-Fock potential.

The strong term dependence of the f-wave channel in the d^9kf and $f^{13}kf$ final-state configurations was accounted for by computing those partial waves separately in term-dependent nonlocal Hartree-Fock potentials for the singlet states. The $d^9kf\ ^1P$ potential is

$$V_{\mathrm{TDHF}}P_{kf}=V_{\mathrm{av}}P_{kf}-[(8/35)Y^2(nd,nd,r)+(2/21)Y^4(nd,nd,r)]P_{kf}$$
$$+[(137/70)Y^1(nd,kf,r)-(2/105)Y^3(nd,kf,r)-(5/231)Y^5(nd,kf,r)]P_{nd} \quad (5)$$

and the $f^{13}kf\ ^1S$ potential is

$$V_{\mathrm{TDHF}}P_{kf}=V_{\mathrm{av}}P_{kf}-[(4/15)Y^2(nf,kf,r)+(2/11)Y^4(nf,kf,r)+(100/429)Y^6(nf,nf,r)]P_{kf}$$
$$+[(195/14)Y^0(nf,kf,r)-(2/105)Y^2(nf,kf,r)-(1/77)Y^4(nf,kf,r)-(1/77)Y^6(nf,kf,r)]P_{nf}\ , \quad (6)$$

where $Y^k(nl,kl',r)$ is

$$Y^k(nl,kl',r)=(1/r^{k+1})\int P_{nl}(x)x^kP_{kl'}(x)dx+r^k\int P_{nl}(x)(1/x^{k+1})P_{kl'}(x)dx \quad (7)$$

and V_{av} is the configuration-averaged potential for the valence-electron—subshell interaction.[7]

For d^{10} subshell ionization, ground-state correlation of the type $d^{10}+d^8f^2$ was included in the initial state in the manner described by Pindzola *et al.*[17] The six terms contributing to the ^1S term were computed using the multiconfiguration method of Fischer.[15] The scattering matrix element including the correlation contribution M_{corr} is

$$M_{\mathrm{corr}}(k_i4d,k_fk_e)=c_1M(k_i4d,k_fk_e)$$
$$+c_2L(4f,k_e)M(k_i4d,k_f4f)\ , \quad (8)$$

where $M(k_i4d,k_fk_e)$ is the uncorrelated matrix element, $L(4f,k_e)$ is the overlap between the $4f$ correlation orbital and the k_e ejected wave, and $M(k_i4d,k_f4f)$ is the matrix element corresponding to excitation of a $4d$ core orbital to a $4f$ correlation orbital. c_1 and c_2 are the configuration mixing coefficients. It is interesting to note that ground-state pair correlations affect the total ionization cross section by means of the nonzero overlap between the term-dependent ejected f waves and the compact $4f$ correlation orbitals.

III. RESULTS

A. Xenonlike ions: 4d subshell ionization

Figures 2—5 present distorted-wave Born-exchange cross sections for electron-impact ionization of a $4d$ electron in Xe, Cs^+, Ba^{2+}, and La^{3+}. The cross sections are given in units of πa_0^2 and the incident electron energy u is expressed in units of the ionization energy

$$u=E_i/I\ , \quad (9)$$

where E_i is the incident electron and I is the ionization energy of the subshell being ionized. Ionization of a $4d$ electron in xenonlike ions leaves the residual ion in a singly autoionizing configuration resulting in effective double ionization of the target by a single electron impact. The relevant experimental data used for comparison purposes will thus be that for double ionization of the target by a single electron impact. In comparing distorted-wave theory with experiment we have neglected the contribution to the double ionization cross section due to direct double ionization. This is a higher-order process involving at least two two-electron interaction operators, and has not yet been studied quantum mechanically. Although some very simple classical approximations[18] have been proposed to describe this process, they are of such a crude nature that they would add little to the present comparison of theory and experiment.

Several theoretical curves are shown for each ion. The solid curve corresponds to the most elaborate calculation, in which the ejected f wave is computed in the term-dependent Hartree-Fock potential for the $4d^95s^25p^6kf\ ^1P$ channel and ground-state correlation is included in the initial state. The long-dashed curve corresponds to a Born-exchange calculation in which all partial waves were computed in semiclassical exchange potentials (i.e., no term dependence). The short-dashed curve is a semiclassical exchange partial-wave calculation which neglects scatter-

ing exchange. Several additional calculations are shown for Cs^+ to illustrate the association of the scattering resonance with the scattered electron channel. In xenonlike ions the resonance appears only when distorted waves are employed in the *scattered* electron channel.

For neutral xenon (Fig. 2) the cross section computed with SCE partial waves shows a very pronounced feature at $u=1.75$ corresponding to a resonance in the scattered electron channel. A second maximum, associated with the ejected channel, occurs at $u=5$. It is this second maximum that corresponds to the usual maximum in the cross section. When term-dependent ejected f waves are used in the calculation, both of the peaks in the Xe cross section are considerably reduced. The scattered electron channel resonance at $u=1.75$ remains, however, as a sharp increase in the cross section near threshold. The effect of ground-state correlation on the cross section is an almost constant 10% reduction of the term-dependent potential result over the entire energy range considered here.

Also shown in Fig. 2 are the experimental data of Stephan and Mark[19] for double ionization of Xe. Comparison of theory with experiment reveals two principal disagreements. First, the onset of double ionization appears to occur at the threshold for double ionization of the $5p$ subshell, i.e., for the process $4d^{10}5s^25p^6 \rightarrow 4d^{10}5s^25p^4$ which has a threshold of 1.2 a.u. compared to the calculated Hartree-Fock $4d$ subshell ionization energy of 2.58 a.u. Thus it appears that there is an additional process for double ionization beyond inner-shell ionization. The abrupt break in the experimental data at $u=1$, however, indicates that once the threshold for inner-subshell ionization is reached the ionization plus autoionization process is an important contribution to the total cross section. The second major disagreement between theory and experiment for Xe is the apparent overestimate of the cross section by distorted-wave theory at high energy. Although the measurements indicate a decrease in the cross section as the incident electron energy surpasses the resonance, the calculated cross section decreases only slightly before reaching a second maximum. The sensitivity of the cross section to the partial-wave potentials suggests that the distorted-wave approximation as applied here may not fully account for the complex structure occurring in the continuum channels of such a heavy atom. In the distorted-wave approximation the scattering states are computed in the potential of the neutral ground state with no provision for polarization of the target. Better results might be expected from theories which allow a more complex treatment of the scattering electron—target-atom interaction. (The ejected channel should be less susceptible to such problems, since it acts under a unit asymptotic charge. Calculations of the $4d$ *photo*absorption spectrum[17] using term-dependent ejected f waves yield cross sections in reasonable agreement with experiment and with other theoretical methods such as the random-phase approximation, indicating that the bound-orbital—ejected-electron interaction is treated reasonably well.)

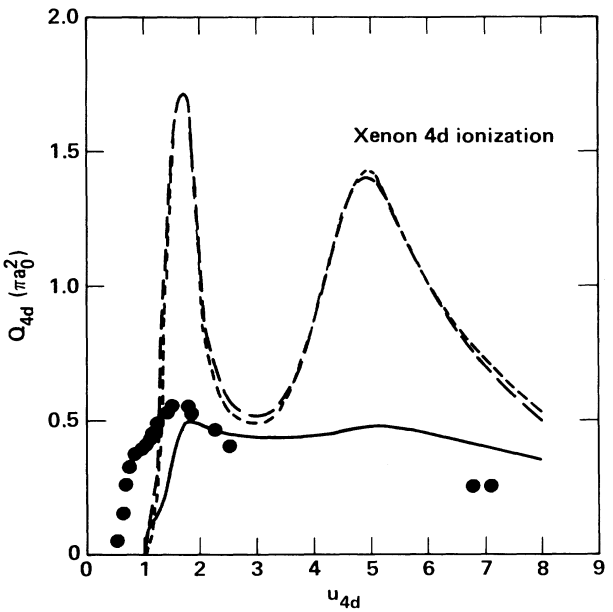

FIG. 2. Cross section for electron-impact ionization of the $4d$ subshell in neutral xenon ($I_{4d}^{HF}=2.584$ a.u.). ——, distorted-wave Born exchange including term-dependent ejected f waves and no ground-state correlation. ———, distorted-wave Born exchange with semiclassical exchange-approximation partial waves and ground-state correlation. ---; same as dashed curve but without scattering exchange. ●: measurements of Stephan and Mark (Ref. 19).

It is not surprising, based on these arguments, that our predictions for the cross sections of ions are in much better agreement with the observed data than is the case for neutral Xenon. In Cs^+ (Fig. 3) the distorted-wave cross section contains a very large and relatively narrow resonance at $u=1.35$ which is in good agreement in both amplitude and shape with the measurements of Hertling *et al.*[20] Also shown in Fig. 3 are the results of several other calculations of the $4d$ cross section of Cs^+ made using various combinations of $Z=1$ Coulomb waves and SCE distorted waves as scattering states. The object of this comparison is to demonstrate that the resonance is associated with the *scattered* electron channel rather than the incident or ejected channels. The resonance structure at low incident electron energies only occurs when distorted waves are used to describe the *scattered* electron. That the resonance is in the scattered kf channel is also apparent from the phase shift for kf partial waves for Cs^+ shown in Fig. 1. The threshold energy for ionization of a $4d$ electron is already beyond the range of the shape resonance, so the incident channel cannot participate. In the ejected channel the effect of the potential barrier is reduced by the presence of the $4d$ hole, preventing the formation of a complete scattering resonance. Examination of the energy differential cross section further confirms that the resonant behavior occurs at a fixed scattered electron energy. The effect of ground-state correlation in Cs^+ was to almost uniformly reduce the term-dependent cross section by about 15%.

Figure 4 presents theoretical cross sections for Ba^{2+}. No measurements are available for this ion, which is un-

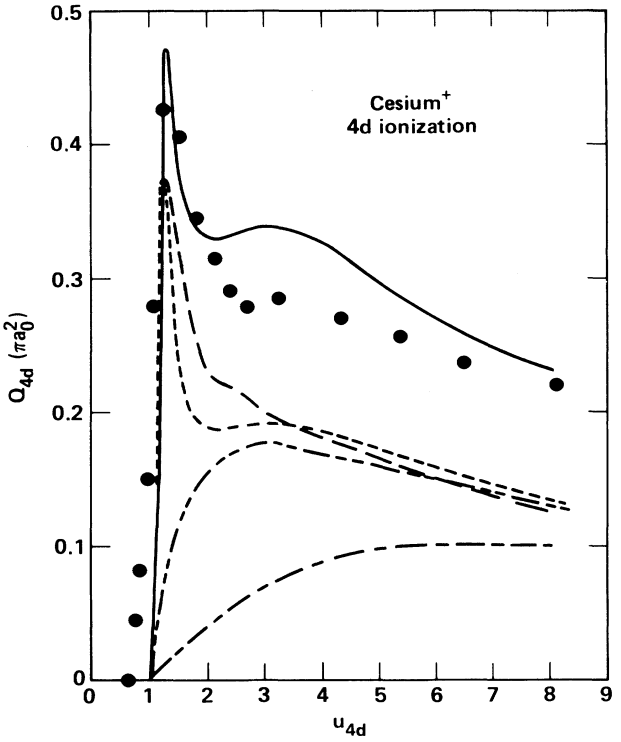

FIG. 3. Cross section for electron-impact ionization of the $4d$ subshell in Cs^+ ($I_{4d}^{HF}=3.387$ a.u.). ——, distorted-wave Born exchange including term-dependent ejected f waves and ground-state correlation. ———, distorted-wave Born exchange with semiclassical exchange-approximation partial waves and no ground-state correlation. --- curve, same as dashed curve but without scattering exchange. —·—·, same as dotted curve but scattered waves are computed in a $Z=1$ Coulomb potential. ——··, same as dotted curve but both incident and scattered waves are computed in a $Z=1$ Coulomb potential. ●: measurements of Hertling *et al.* (Ref. 20).

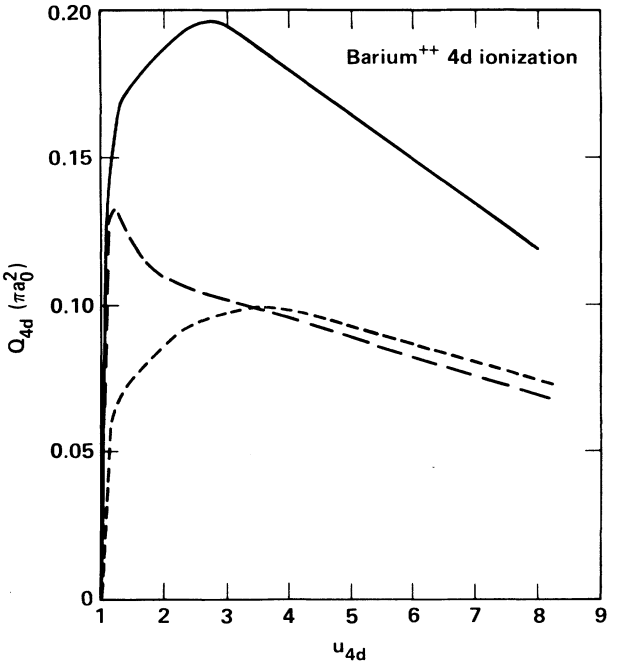

FIG. 4. Cross section for electron-impact ionization of the $4d$ subshell in Ba^{2+} ($I_{4d}^{HF}=4.263$ a.u.). ——, distorted-wave Born exchange including term-dependent ejected f waves and ground-state correlation. ———, distorted-wave Born exchange with semiclassical exhange-approximation partial waves and no ground-state correlation. ---, same as dashed curve but without scattering exchange.

fortunate since different theoretical methods produce qualitative differences in the shape of the cross section. A simple distorted-wave calculation which neglects scattering exchange, term dependence in the ejected channel, and ground-state correlation displays no resonance structures at low incident electron energy. When scattering exchange is included, however, a sharp resonance appears at $u=1.25$, just above threshold. When term-dependent partial waves are employed, the resonance increases in amplitude, and merges with a similarly enhanced main peak in the cross section. The reason that the resonance only occurs only in the exchange cross section follows from the combination of potentials used in the distorted-wave Born-exchange method. For the direct matrix element determining the no-exchange calculation the (slow) ejected electron is computed in the field of the residual ion, which has a stronger asymptotic Coulomb potential and hence a weaker potential barrier than the scattering potential for the initial ion. Although the (fast) scattered electron is computed in the field of the initial ion, the effect of the large potential barrier is offset by the higher energy of the electron. In the exchange matrix elements, however, the potentials are reversed in order to preserve orthogonality between initial and final-state orbitals. The (slow) ejected electron is now computed in the potential of the inital ion and the (fast) scattered electron in the ionic potential. It is the combination of low ejected-electron energy and a stronger potential barrier that causes a resonance to appear in the ejected channel. The additional nonlocal exchange potential occurring in the term-dependent calculation causes the potential barrier in the direct matrix element ejected channel to be enhanced, resulting in significant changes in the term-dependent no-exchange cross section as well.

These hypotheses regarding the ejected-electron channel in Ba^{2+} are supported by calculations on the photoabsorption spectrum of the ion.[21] When term-independent orbitals are employed to compute the $4d$ photoabsorption spectrum, a very small cross section results, since most of the available oscillator strength in the $4d$ subshell is concentrated in the $4d$-$4f$ bound-bound transition. When a term-dependent approximation is employed for the f channel, the $4f$ electron is repelled from the core (it resides in the outer potential well) resulting in a small $4d$-$4f$ oscillator strength. The balance of the oscillator strength is then shifted into the continuum, enhancing the photoionization cross section.

Figure 5 plots the scaled electron ionization cross sec-

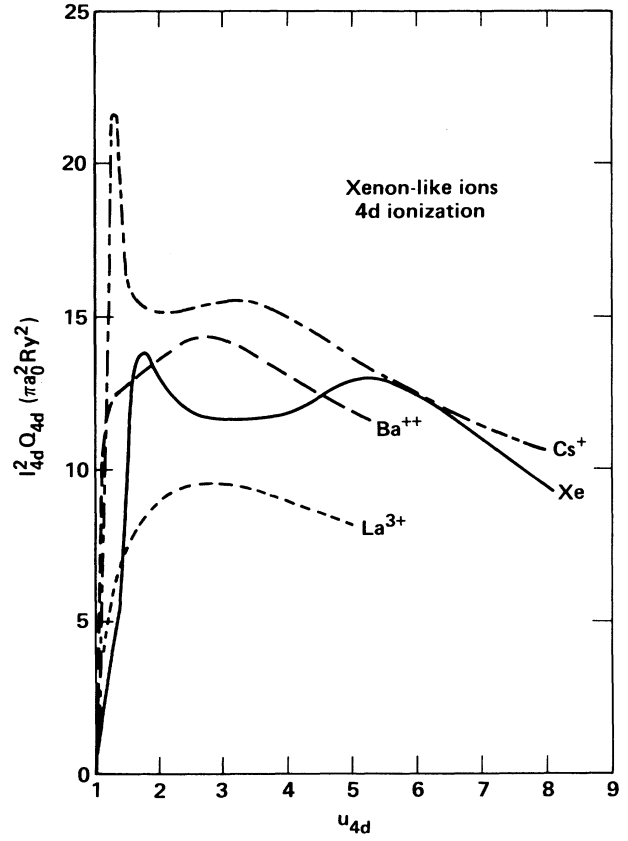

FIG. 5. Comparison of the scaled cross section for electron ionization of the $4d$ subshell of the first four ions of the xenon isoelectronic sequence. As the nuclear charge increases, the scattering resonance moves to lower incident electron energies and becomes narrower.

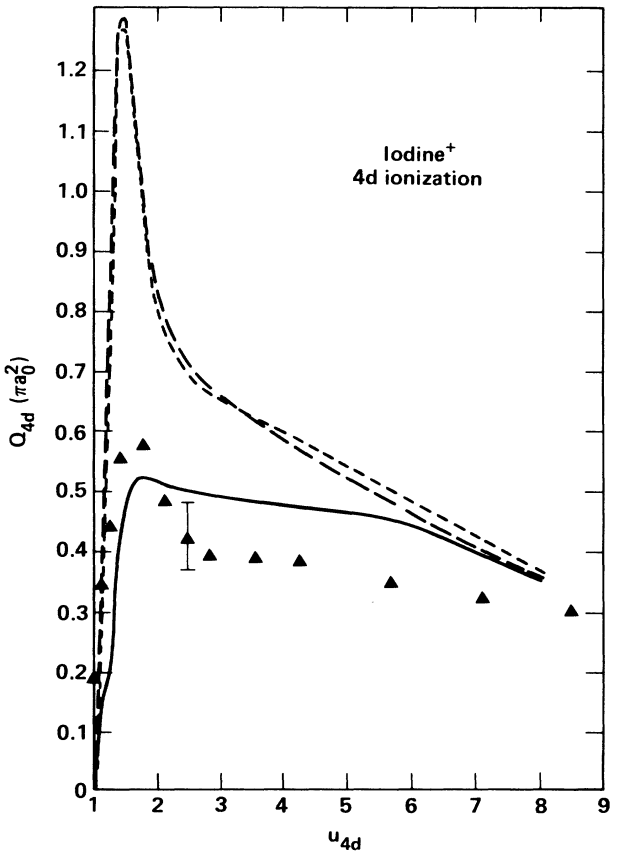

FIG. 6. Cross section for electron-impact ionization of the $4d$ subshell in I^+ ($I_{4d}^{HF}=2.592$ a.u.). ——, distorted-wave Born exchange including term-dependent ejected f waves and ground-state correlation. ——, distorted-wave Born exchange with semiclassical exchange-approximation partial waves and no ground-state correlation. ---, same as dashed curve but without scattering exchange. ▲, measurements of Achenbach *et al.* (Ref. 22).

tion, I^2Q for Xe, Cs^+, Ba^{2+}, and La^{3+}, where I is the ionization energy in rydbergs. As the nuclear charge is increased, the resonance moves to lower scattered-channel energies and becomes sharper. Both of these effects are consistent with the inner-well virtual resonance state approaching zero energy as the depth of the inner potential well increases.[6]

B. $4d$ ionization in Xe^+ and I^+

Xe^+ and I^+ are the only two heavy ions besides Cs^+ for which electron double-ionization measurements are available over the incident electron energy range $u=1-2$. Xe^+ was first studied theoretically by Pindzola *et al.*[17] using almost the same method as ours, with almost identical results. We have extended their calculation to higher energies in order to better illustrate the resonance effect on the cross section. Figures 6 and 7 compare the present theoretical results with the observations of Achenbach *et al.*[22] In both cases the effect of using term-dependent potentials in the ejected channel is to reduce the amplitude of the resonant component of the cross section, quite significantly in the case of I^+. For both ions the term-dependent calculation appears to overcorrect the errors of the SCE approximation in that the observed resonances are larger than those which are calculated. Still, the comparison of distorted-wave theory and experiment is quite favorable for these complex ions and demonstrates that giant resonances in the electron ionization of heavy ions are not a feature peculiar to Cs^+. Note that the apparent contribution due to direct double ionization (indicated by a nonzero cross section below the threshold for $4d$ subshell ionization) is much weaker for Xe^+ than for neutral Xe. This is consistent with the hypothesis of Pindzola *et al.*[17] who studied $4d$ ionization of Xe^{n+} ions and concluded that the principal double-ionization mechanism for multiply charged heavy ions is inner-shell ionization followed by autoionization, rather than direct double ionization.

It is of interest to find if giant resonances are restricted to $d\rightarrow f$ transitions, or whether they occur for other subshell symmetries as well. For this reason we have per-

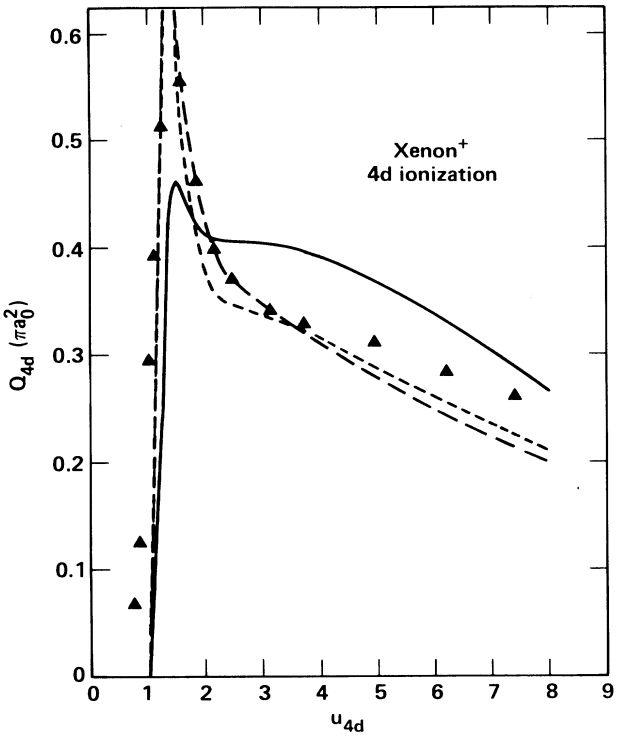

FIG. 7. Cross section for electron-impact ionization of the $4d$ subshell in Xe^+ ($I_{4d}^{HF}=2.976$ a.u.). ——, distorted-wave Born exchange including term-dependent ejected f waves and ground-state correlation. ———, distorted-wave Born exchange with semiclassical exchange-approximation partial waves and no ground-state correlation. ---, same as dashed curve but without scattering exchange. ▲, measurements of Achenbach *et al.* (Ref. 22).

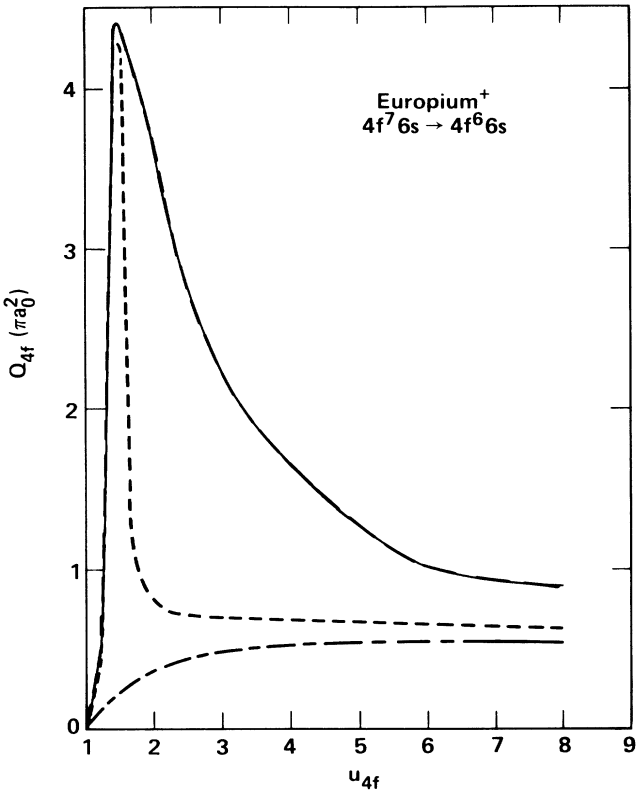

FIG. 8. Cross section for electron-impact ionization of the $4f$ subshell in Eu^+ ($I_{4f}^{HF}=0.6019$ a.u.). ——, distorted-wave Born-exchange calculation. ———, distorted wave without exchange. ——-, Coulomb-Born calculation without exchange. The resonance only appears when distorted waves are used to describe the scattered-electron channel. The effect of scattering exchange is to broaden the resonance to higher energies.

formed preliminary calculations of electron-ionization cross sections for a variety of heavy ions, most notably several rare-earth ions.

C. Eu^+ 4*F* subshell ionization

The ground configuration of Eu^+ is $4f^7 6s$. Figure 8 shows the result of an SCE partial-wave calculation for $4f$ ionization in Eu^+, i.e., the transition $4f^7 6s \rightarrow 4f^6 6s$. A resonance in the scattered channel at approximately 0.16 a.u. causes an abrupt and sizable increase in the total cross section at $u=1.25$. This is an increase of more than an order of magnitude compared to the Coulomb-Born cross section, which might be considered as a nonresonant "background" cross section. The effect of scattering exchange is to considerably broaden the narrow resonance present in the direct calculation. As was found for Ba^{2+}, Eu^+ is an example of where an accurate measurement could provide important guidance to theory on appropriate approximations for scattering exchange in complex electron-ionization events.

It was found in all cases where resonances occurred in $4f$ subshell ionization that the $4f$-kf channel dominated the cross section, sometimes with significant resonant contributions from the $4f$-kd channel at lower incident energies. The $4f$-kg dipole channel, which might be expected to be a major component of the cross section, was found to be very weak compared to the monopole channel owing to the very large centrifugal barrier which prevents a close approach of the kg wave to the relatively compact $4f$ subshell. The partial-wave expansions for $4f$ subshell ionization were found to be very rapidly convergent with increasing angular momentum compared to previous experience with the ionization of orbitals with lower l.

Another feature noted for giant resonances in $4f$ subshell ionization was the sharpness of the resonance in the scattered-electron channel. Whereas in $4d$ ionization the scattered channel resonance was quite broad, in the case of $4f$ ionization it was very narrow, necessitating a very fine grid of energy points in the final-state energy distribution. Although a five-point Gaussian integration algorithm was found quite adequate for $4d$ ionization, 20 points were required to span the resonant behavior of the $4f$ energy differential cross section.

D. Ionization of the $4f^{14}$ subshell

Figure 9 presents calculated cross sections for ionization of the $4f^{14}$ configuration in Tm^+. Although $4f^{14}\,{}^1S$ is actually an excited state in Tm^+ (the ground state is $4f^{13}6s$), we include it as an interesting illustration of giant resonance effects in rare-earth ions with simple initial and ionic configurations. Also, this state is expected to be well populated in both plasma and ion beam sources of Tm^+ ions.

The results of the distorted-wave Born (no scattering exchange) and the Born-exchange calculations for Tm^+ are similar, displaying a sharp resonance at $u=2$ and a much larger and broader maximum at $u=3.25$. The shape resonance in Tm^+ occurs at 0.5 a.u. for a semiclassical exchange potential approximation. This is a low enough energy that both the incident and scattered waves are participants. The sharp feature at $u=2$ is a resonance in the incident channel, whereas the enhancement at $u=4$ is at least partly due to the scattered-electron channel. When term-dependent kf ejected waves are employed, the low-energy incident channel resonance remains and the second maximum is considerably reduced and broadened to higher incident electron energy. Note that the term-dependent cross section has not peaked even at $u=8$, the highest incident electron energy considered here.

Figure 10 compares scaled SCE cross sections, I^2Q, for Tm^+ with similar calculations for the isoelectronic ions Yb^{2+} and Lu^{3+}. Neither of the higher Z ions display resonant behavior in the total cross section, although the

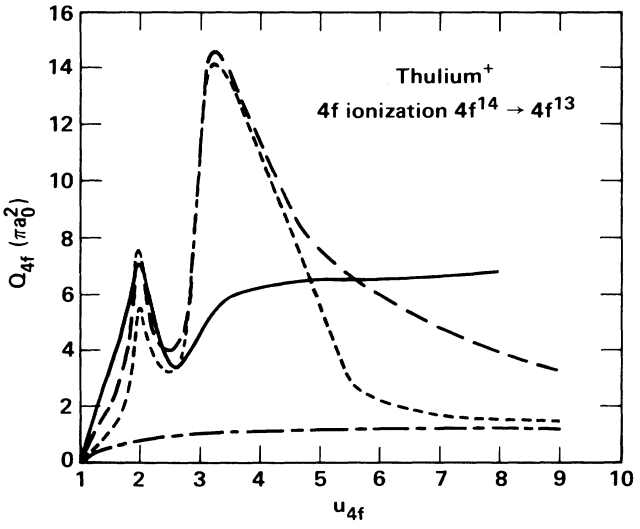

FIG. 9. Cross section for electron-impact ionization of the $4f$ subshell in Tm^+ ($I^{HF}_{4f}=0.2560$ a.u.). ——, distorted-wave Born-exchange including term-dependent ejected f waves. – – –, distorted-wave Born-exchange with semiclassical exchange-approximation ejected waves. ---, same as dashed curve but without scattering exchange. —·—·—, Coulomb-Born calculation without exchange. The resonance appears in all of the distorted-wave calculations.

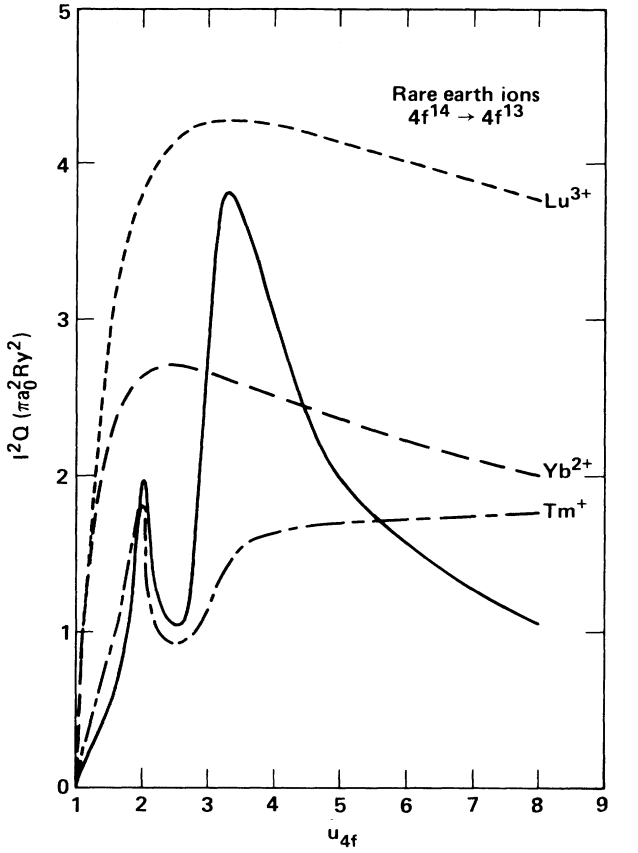

FIG. 10. Scaled electron-ionization cross sections for the first three ions of the $4f^{14}\,{}^1S$ isoelectronic sequence computed with semiclassical exchange-approximation partial waves. [$I^{HF}_{4f}(Tm^+)=0.2560$ a.u., $I^{HF}_{4f}(Yb^{2+})=0.9261$ a.u., $I^{HF}_{4f}(Lu^{3+})=1.771$ a.u.]. A scattering resonance only appears for the first ion in the sequence.

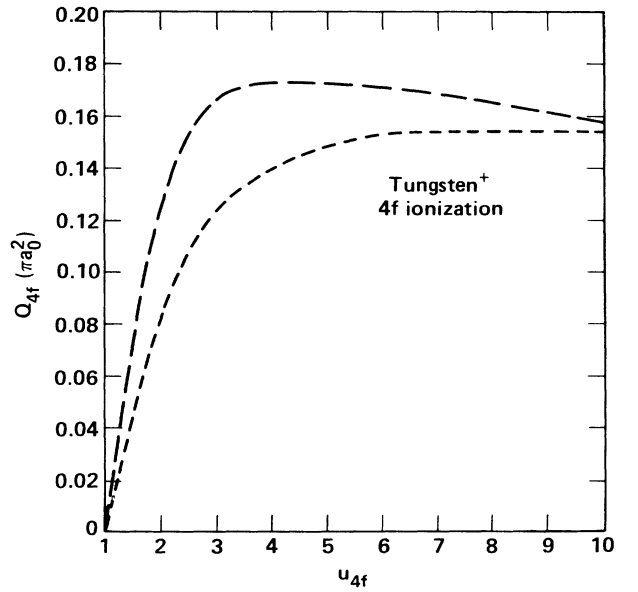

FIG. 11. Cross section for electron-impact ionization of the $4f$ subshell in W^+ ($I^{HF}_{4f}=2.101$ a.u.). – – –, distorted-wave Born-exchange calculation. ---, distorted-wave without exchange.

peak cross section in Yb^{2+} occurs at significantly lower energy than it does for Lu^{3+}.

In order to determine if additional screening electrons would cause a reappearance of resonant behavior at higher Z, an SCE partial-wave calculation was performed for the $4f^{14}5s^25p^65d^46s \rightarrow 4f^{13}5s^25p^65d^46s + e^-$ cross section in W^+. The results, shown in Fig. 11, show no evidence of resonant behavior.

IV. DISCUSSION

The appearance of giant scattering resonances in high-angular-momentum partial-wave channels has been shown to have a profound effect on the near-threshold behavior of the electron-impact ionization cross section for heavy neutral and few-times-ionized atoms. Such resonance structures have been identified in a variety of ions and affect both single and double ionization.

Several inferences concerning the dynamics of electron-impact ionization from complex heavy ions can be drawn from these calculations. First, the good agreement between the present distorted-wave calculations and available experimental data for the double ionization of heavy ions by a single electron impact implies that inner-shell ionization followed by autoionization is a dominant mechanism for multiple ionization in such systems. Only for Xe I is there a substantial contribution from direct double ionization. This result is in agreement with the earlier work of Pindzola *et al.*[17] who studied ionization of Xe^{n+} ions. Note, however, that the different Z scaling of the autoionization rate (roughly constant with Z) and the radiative decay rate for the intermediate state (which scales as Z^4) implies that at very high Z radiative stabilization of the intermediate state may occur, interrupting the autoionization event. Combined with the apparent decreasing contribution of direct multiple ionization for increasing ionic charge, one then expects the multielectron ionization rate to decrease somewhat for very highly charged heavy ions. The degree of this reduction in multiple ionization will of course depend on the detailed atomic structure of the ion, i.e., the selection rules governing radiative decay and autoionization. For example, if a particular intermediate autoionizing state is metastable with respect to photon emission, there may still be a substantial multiionization cross section.

A second conclusion which might be drawn from the present comparison of theory and experiment is the apparent isolation of the final-state channels in the ionization event. For I^+, Xe^+, and Cs^+ the location and shape of the resonance is predicted well using partial waves computed in the potential of the *initial* target state. It was found from studying the phase shifts for orbitals computed in the potential of the residual ion ($4d^95s^25p^n$) that this potential often does not support a resonance. This implies that the ionization event is either a *slow* process compared to the duration of the scattering interaction (i.e., the bound-continuum transition occurs in a "transition potential" generated by the scattering electron) or that the autoionization process is fast enough that the scattered electron actually sees a full $4d^{10}$ subshell which can support the formation of a shape resonance. In the former picture the scattered partial wave sees the initial target potential and in the latter it sees the $4d^{10}5s^25p^{n-1}$ configuration with some additional contribution due to the ejected electron. These alternate descriptions of the final scattered wave may be distinguished by comparing the autoionization rate of the residual ion A_a with the time spent by the scattering electron in the vicinity of the ion t_s. For a resonance occurring at 0.6 a.u. scattered-electron energy the electron velocity is $\sqrt{E/2m_e} = 1.2 \times 10^8$ cm/sec. Taking the size of the ion as $1a_0 = 0.529 \times 10^{-8}$ cm, we find that $t_s = 4.4 \times 10^{-17}$ sec. This crude analysis implies that the scattering event is much faster than typical rearrangement times of the residual ion and that at most a single-electron emission occurs during the duration of the ionizing collision.

It is interesting to note that the existence of the resonance is strongly determined by the core-scattered electron interaction. The interaction of the two final-state continuum electrons is apparently insufficient to destroy the resonance. This is in agreement with the results of many studies of electron ionization in light ions and atoms[2,8] where the scattering-electron—target interaction is less complicated but the continuum-continuum interaction is formally the same. In all of these cases good agreement between theory and experiment was obtained by optimizing the description of the continuum-target interaction. This implies, at least at the gross level of the total ionization cross section, that the final-state continuum-continuum interaction is a relatively minor contribution to the ionization event. An exception to this pattern is electron scattering from complex neutral atoms, where the absence of a strong long-range potential in the continuum channel makes the scattering event much more sensitive to screening effects. Also, one expects that the angular distribution of the scattered and ejected electrons will be more sensitive to the continuum-continuum interaction than the integrated cross section since the former is a more direct probe of individual scattering matrix elements.

The separate-channel nature of shape resonances in heavy-ion ionization implies that multiple resonances may occur in the same ion, i.e., a separate resonance may occur in each of the incident, scattered, and ejected channels. Tm^+ is an example of separate resonances in the incident and scattered channels. Such cases offer especially interesting probes of electron-atom interactions in that each channel is distinguished even at the level of the total cross section.

Since shape resonances result from a delicate competition between several terms in the atomic wave equation, it is difficult to predict where they will occur without actually calculating the continuum phase shifts. Nevertheless, one can bound their occurrence to those systems suspected of supporting robust double-well potentials describing high-angular-momentum partial waves. In particular, singly charged ions in the vicinity of xenon and radon appear especially promising. The complex structure of the f shells in the lanthanide and actinide ions should also support strong, perhaps multiple, resonance structures. Many of the neutral atoms in this region may also contain resonance structures. So far Ba^{2+} is the only multiply

charged ion which is predicted to exhibit pronounced resonantlike behavior in electron-impact ionization, although additional investigations of heavier ions or ions initially in excited states may reveal other examples. Measurements and calculations of the double-ionization cross sections of xenon ions appear to show distinct resonant behavior only in the singly charged ion.[17] Note that resonances are not necessarily restricted to the ionization of high-angular-momentum orbitals. Since resonances typically occur in the *scattering* channels, they will affect *all* scattering processes involving those partial waves. Also, even though an ion may not support a full resonance (phase shift of a complete π), there may still be significant potential-related "enhancements" of the cross section. Such is the case in electron-impact ionization of the palladium isoelectronic sequence, where the nonresonant but double-well potential describing the ejected kf waves results in large changes in the shape of the cross section even for multiply charged ions.[11]

Although experimental data already exists for a sufficient number of heavy atoms to show that giant resonances are not an isolated phenomenon in electron-impact ionization, one can identify several areas where additional measurements would greatly improve our understanding of this process. Observation of the low-energy ionization cross section of Ba^{2+} would be very helpful in unraveling the role of electron exchange among the final-state continuum electrons. The existence of a resonance in this ion depends critically on the energy-dependent distribution of the cross section in the final state. Although measurement of the total cross section would provide the essential information, observation of the single differential cross section $\partial Q/\partial E$, where E is the energy of the scattered electron, would even more precisely identify the resonance.

A second important experimental study of giant resonances in electron ionization would be measurements of rare-earth ions. These are especially interesting systems in that distorted-wave theory predicts the existence of multiple resonances. Also, calculated cross sections for such ions are especially sensitive to the details of the target atomic structure and scattering-exchange approximations.

It is clear that such large features in the electron-ionization cross section of heavy atoms and ions will have significant effects on the ionization balance of high-Z, low-temperature plasmas. The resonant enhancement of the single- and double-ionization cross sections at low energies will cause an increase in the effective charge of the plasma as well as a modification of the three-body recombination rate[23] (the inverse process for electron-impact ionization). Müller has recently reported the results of kinetics modeling studies of xenon plasmas and has found dramatic changes in the ionic populations derived from atomic models with and without multiple ionization.[24]

While the present study has concentrated on giant resonances in electron-impact *ionization,* similar processes are expected to occur for electron-impact *excitation.* Strong enhancements to such cross sections are expected to occur whenever d- or f-wave shape resonances occur. Resonances in the electron-excitation cross section will lead to higher plasma radiative cooling rates. Furthermore, the existence of strong resonances in the electron-excitation cross section suggests consideration of this mechanism as a candidate for a low-temperature electron-beam-pumped x-ray laser.

The sensitivity of the inelastic scattering cross sections of heavy ions to partial-wave potentials strongly urges the undertaking of additional selected measurements and calculations of both excitation and ionization. These additional data will provide valuable insight not only into the scattering potentials governing the formation of the resonances, but also the validity of the approximation employed for the phase of the scattering-exchange matrix element—a fundamental ambiguity in the Born-exchange theory of electron-impact ionization.

ACKNOWLEDGMENTS

I would like to thank M. S. Pindzola of Auburn University for several valuable discussions. Work was performed under the auspices of the U.S. Department of Energy by Lawrence Livermore National Laboratory under Contract No. W-7405-Eng-48.

[1]N. F. Mott and H. S. W. Massey, *The Theory of Atomic Collisions* (Oxford University Press, Oxford, 1965).
[2]G. H. Dunn, in *Electron Impact Ionization,* edited by T. D. Mark and G. H. Dunn (Springer-Verlag, Wein, 1985), Chap. 3.
[3]S. M. Younger, Phys. Rev. Lett. **56**, 2618 (1986).
[4]D. R. Hartree, Proc. Cambridge Philos. Soc. **24**, 89 (1927).
[5]R. I. Karaziya, Usp. Fiz. Nauk **135**, 79 (1981) [Sov. Phys.—Usp. **24**, 775 (1981)].
[6]J. P. Connerade, J. Phys. B **17**, L165 (1984).
[7]E. U. Condon and H. Odabasi, *Atomic Structure* (Cambridge University Press, Cambridge, 1980).
[8]S. M. Younger, Phys. Rev. A **22**, 2682 (1980).
[9]D. J. Kennedy and S. T. Manson, Phys. Rev. A **5**, 227 (1972).
[10]M. S. Pindzola, D. C. Griffin, and C. Bottcher, Phys. Rev. A **27**, 2331 (1983).
[11]S. M. Younger, Phys. Rev. A **34**, 1952 (1986).
[12]S. M. Younger, Phys. Rev. A **22**, 111 (1980).
[13]S. M. Younger, Phys. Rev. A **23**, 1138 (1981).
[14]R. K. Peterkop, Zh. Eksp. Teor. Fiz. **41**, 1938 (1961) [Sov. Phys.—JETP **14**, 1377 (1962)].
[15]C. F. Fischer, *The Hartree-Fock Method for Atoms* (Wiley, New York, 1977).
[16]M. E. Riley and D. G. Truhlar, J. Chem. Phys. **63**, 2182 (1975).
[17]M. S. Pindzola, D. C. Griffin, and C. Bottcher, J. Phys. B **16**, L355 (1983); M. S. Pindzola, D. C. Griffin, D. H. Crandall, R. A. Phaneuf, and D. C. Gregory, Phys. Rev. A **29**, 1749 (1984).
[18]M. Gryzinski, Phys. Rev. **138**, 336 (1965).
[19]K. Stephan and T. D. Mark, J. Chem. Phys. **81**, 3116 (1984).
[20]D. R. Hertling, R. K. Feeney, D. W. Hughes, and W. E.

Sayle, J. Appl. Phys. **53**, 5427 (1982).
[21]T. B. Lucatorto, T. J. McIlrath, J. Sugar, and S. M. Younger, Phys. Rev. Lett. **47**, 1124 (1981).
[22]Ch. Achenbach, A. Müller, and E. Salzborn, Phys. Rev. Lett. **50**, 2070 (1983).
[23]I. A. Sellin, private communication.
[24]A. Müller, Phys. Lett. **113A**, 415 (1986).